

## Impact of Grey Particles Multiplicity on the Characteristics of Particles Produced in 4.5 AGeV/c $^{12}\text{C}$ -Nucleus Interactions

Khushnood Husain<sup>1</sup>, Prithipal Singh<sup>1</sup>, Praveen Prakash Shukla<sup>2</sup> and M. Saleem Khan<sup>2</sup>

1-University Polytechnic, Jamia Millia Islamia New Delhi-110025

2-Department of Applied Physics, MJPR, University Bareilly-243001

**Abstract:** An attempt has been made to study the dependence of various characteristics of relativistic charged particles, produced in 4.5 A GeV/c  $^{12}\text{C}$ - nucleus interactions on the multiplicity of grey particles. The results reveal that the peaks on  $\eta$ -distributions shift towards the smaller values of  $\eta$  with increasing multiplicity of grey particles. The results also reveal that the value of mean normalized pseudo rapidity density is less than unity in the projectile fragmentation region; while the value of this parameter is found to increase in the target fragmentation region. Finally, it is observed that the clusterization of final state relativistic charged particles occurs significantly in 4.5 A GeV/c  $^{12}\text{C}$ -nucleus reactions.

**Keywords:** relativistic charged particles, pseudo rapidity, projectile and target fragmentation region, clusterization

### I. Introduction

Angular characteristics of relativistic charged particles produced in high-energy hadron-hadron and hadron-nucleus collisions have been extensively investigated by several workers [1-5]. However, little attention is paid to investigate the same in relativistic heavy-ion interactions [6-9] even though angular characteristics of relativistic charged particles produced in nucleus-nucleus interactions remain the most statistically reliable source of information about the single particle distributions in multi-particle production in such reactions.

In present work, we have presented the results on the angular characteristics of relativistic charged particles produced in  $^{12}\text{C}$ -nucleus interactions at 4.5 A GeV. These angular characteristics are investigated in terms of the pseudorapidity variable,  $\eta = [-\ln \tan (\theta/2)]$ , where  $\theta$  is the angle of emission of secondary charged particle in the lab system. We have investigated the dependence of angular characteristics on multiplicity of grey particles to draw some useful conclusions.

### II. Experimental details

All the relevant information regarding emulsion stacks, scanning procedure, selection criteria and method of measuring the angles etc. may be found in our earlier publications [10-12].

For investigating the angular characteristics of relativistic charged particles, a random sample of 681 disintegrations caused by 4.5 A GeV carbon nuclei in nuclear emulsion was analyzed. The secondary charged particles produced in each interaction are classified into grey, black and relativistic charged particles. Tracks having ionization in the interval  $1.4g_0 - 10g_0$  are termed as grey tracks, where  $g_0$  represents the plateau ionization. Track with ionization greater than  $10g_0$  is referred to as black track, while relativistic charged particle tracks have ionization less than  $1.4g_0$  respectively. The number of grey, black and relativistic charged particles produced in an event are denoted by  $N_g$ ,  $N_b$  and  $N_s$  respectively.

Furthermore, grey and black tracks taken together are referred to as heavily ionizing tracks in an interaction and their number is denoted by  $N_h = (N_g + N_b)$ .

### III. Experimental results

It is reported [13-15] that number of grey particles,  $N_g$  produced in an interaction may be taken as a good measure of the number of encounters made by the projectile inside the struck nucleus. It is also reported that disintegrations having  $N_g > 3$  are due to interactions with heavy emulsion nuclei [16]. Thus,  $N_g$  is related reasonably well to the atomic mass of the target nuclei and the number of encounters made by the projectile inside the struck nucleus. Thus, for investigating the dependence of pseudorapidity distribution of relativistic charged particles on  $v$ , and size of the target nucleus. We have arranged the experimental data in different  $N_g$  bins, i.e.  $N_g = 0, 1, 2-3, 4-5, 6-8$ , and  $> 9$ .

### 3.1 Dependence of angular distribution of relativistic charged particles on $N_g$

Angular distributions of relativistic charged particles for different  $N_g$  bins are shown in Fig.1. It is seen in the figure that behavior of angular distributions is almost the same and prominent peaks are observed at smaller values of  $\theta$ . Angular distributions of relativistic charged particles having angle,  $\theta < 8^\circ$ , are shown in Fig. 2 for all  $N_g$  bins. It is quite clear from the figure that prominent peaks also exist in the range of very small angle. This may be due to well known phenomenon of proton stripping, superimposed over the uniform distributions. Similar results are also observed by Abd Allah et al [8].

Furthermore, the front/back ratios of the relativistic charged particles in different groups of  $N_g$  have been computed and are displayed in Table 1. It may be seen from the table that the front/back ratio is almost the same for all the groups of  $N_g$ , except for the bin  $N_g = 0$ . Results further indicate that angular characteristics of relativistic charged particles depend on both target size and number of encounters made by the projectile inside the struck nucleus.

### 3.2 Dependence of $\eta$ -spectra on $N_g$

We also studied the dependence of  $\eta$ -distributions of relativistic charged particles on  $N_g$ . The  $\eta$ -distributions for different  $N_g$  bins are displayed in Fig. 3. From this figure, we observed that the peak of distribution shifts towards the lower value of  $\eta$  with increasing  $N_g$  and the  $\eta$ -distribution becomes flatter with increasing value of  $N_g$ . It is further seen in the figure that, the behavior of  $\eta$ -distributions for different target thickness is almost similar to those obtained in the case of high-energy hadron-nucleus collisions [13-15]. This result is in nice accord with the prediction of coherent tube model [17]. It may also be seen from the figure that the width of  $\eta$ -spectra decreases with increasing value of  $N_g$ .

### 3.3 Dependence of $\langle \eta \rangle$ distribution on $N_g$

In order to study the dependence of  $\langle \eta \rangle$ -distributions on the number of grey particles,  $N_g$ , we have estimated the average value of  $\eta$  for each event by using the following relation.

$$\langle \eta \rangle = 1/N \sum_{i=1}^N \eta_i$$

Where N denotes the number of relativistic charged particles in an event.  $\langle \eta \rangle$ -distributions for different  $N_g$  bins are plotted in Fig. 4. It is observed from the figure that peak of the distribution shifts towards the lower value of  $\langle \eta \rangle$  with increasing  $N_g$ . This result may be explained in terms of the fact that relativistic charged particles with large angles would appear in the target fragmentation region. A similar result has been reported by Ahmad et al [18] in the case of nucleus-nucleus reactions at same projectile energy. It is further noted in the same figure, that the distribution becomes narrower as the value of  $N_g$  increases and the height of the plateau also increases with increasing value of  $N_g$ .

### 3.4 Dependence of D ( $\eta$ ) distributions on $N_g$

Berger et al [19] have suggested that rapidity dispersion parameter for individual events can be used to measure the clustering of produced particles along the longitudinal rapidity axis at higher energies. They also reported that events having  $D(\eta) < 0.9$  correspond to the production of a single isotropic cluster. To study the observed behavior, we have calculated the dispersion, D ( $\eta$ ) for each event using the following relation

$$D(\eta) = [\langle \eta^2 \rangle - \langle \eta \rangle^2]^{1/2}$$

Dependence of D ( $\eta$ )-distributions on  $N_g$  is displayed in Fig. 5. It is evidently clear from the figure that maxima of D ( $\eta$ )-distribution shifts towards smaller value of D ( $\eta$ ) with increasing value of  $N_g$ . This result suggests that D ( $\eta$ ) in 4.5 A GeV  $^{12}\text{C}$ -nucleus interactions strongly depends on both, the number of encounters made by the projectile inside the target nucleus, and the size of the target nucleus. The percentages of events having  $D(\eta) < 0.9$  for different  $N_g$  bins are given in Table 2. Based on this observation, we may conclude that clusterization effect occurs significantly in all the categories of interactions considered in the present work.

### 3.5 Dependence of rapidity width on $N_g$

For studying the dependence of the rapidity width, R ( $\eta$ ) on the multiplicity of grey particles, we have calculated the values of R ( $\eta$ ) for each event. Rapidity width R ( $\eta$ ) may be defined as

$$R(\eta) = \eta_2 - \eta_1$$

Where  $\eta_1$  and  $\eta_2$  are respectively the minimum and maximum rapidity in an event.  $\eta$  - distributions for different  $N_g$  bins are displayed in Fig. 6. It is evidently clear from the figure that the peak of  $\eta$ -distribution shifts towards the lower value of  $R(\eta)$  with increasing value of  $N_g$ . This might be due to the fact that the relativistic charged particles produced with relatively larger angle would tend to appear in the target fragmentation region. It may further be noted from the same figure that the space occupied by relativistic charged particles increases with increasing value of  $N_g$ .

### 3.6 Dependence of $d\eta$ -distribution on $N_g$

We also studied the dependence of  $d\eta$ -distribution on  $N_s$  and  $d\eta$  is defined as

$$d\eta = \frac{1}{N_{BA}} \frac{dN_{BA}}{d\eta} - \frac{1}{N_{BN}} \frac{dN_{BN}}{d\eta}$$

where  $\frac{1}{N_{BA}} \frac{dN_{BA}}{d\eta}$  denotes the number of relativistic charged particles per event in nucleus-

nucleus interactions and  $\frac{1}{N_{BN}} \frac{dN_{BN}}{d\eta}$  represents the number of relativistic charged particles

having  $N_h = 0,1$  per event in nucleus-nucleus collisions at the same projectile energy and  $d\eta$ -distributions for different  $N_g$  bins are exhibited in Fig. 7. It may be observed from the figure that  $d\eta$ -distributions are almost similar for all the groups of  $N_g$  considered in present investigation. According to Energy Flux Cascade Model [20], the centre of  $d\eta$ -distribution should be independent of  $N_g$ . Thus, our findings are in nice agreement with the predictions of this model. It is reported [5] that  $d\eta$ -distribution strongly depends on  $N_g$  in high-energy hadron-nucleus interactions. It may be seen in the figure that for higher value of  $\eta$ , the  $d\eta$ -distribution is negative. This result contradicts the idea of complete passivity of the projectile after its first collision inside the struck nucleus [20]. Similar results have also been observed in case of high-energy particle-nucleus collisions [5].

### 3.7 Variation of $r(\eta)$ -distributions with $N_g$

We have also studied the dependence of normalized pseudorapidity distribution,  $r(\eta)$  defined as,

$$r(\eta) = \frac{1}{N_{BA}} \frac{dN_{BA}}{d\eta} \bigg/ \frac{1}{N_{BN}} \frac{dN_{BN}}{d\eta}$$

on the multiplicity of  $N_s$ . Variation of  $r(\eta)$  with  $\eta$  for different groups of  $N_g$  is plotted in Fig. 8. From this figure it is clear that  $r(\eta)$  varies with  $\eta$  in such a way that larger the value of  $\eta$ , smaller will be the value of  $r(\eta)$ . Moreover, it may be noted that in the high rapidity region,  $r(\eta)$  goes on decreasing below 1.0 as one proceeds from smaller to higher  $N_g$  values.

## IV. Conclusions

The analysis of experimental data for the inelastic interactions of 4.5 A GeV carbon nuclei with nuclear emulsion leads to following conclusions.

1. From the angular distribution of relativistic charged particles, we get an indication of limiting fragmentation hypothesis.
2. The front/back ratio of the relativistic charged particles is nearly same for all the groups of  $N_g$ , except  $N_g = 0$ .
3. The maxima of  $\eta$ -spectra are found to shift towards smaller values of  $\eta$  with increasing value of  $N_g$ .
4. The rapidity dispersion distributions clearly indicates the occurrence of clusterization in  $^{12}\text{C}$ -emulsion interactions in all groups of  $N_g$ .
5.  $D(\eta)$ -distribution is observed to remain almost the same with increasing value of  $N_g$ .
6. The behavior of  $\langle n \rangle$ -distribution depends strongly on  $N_g$ .
7.  $d\eta$ -distributions are observed to remain almost constant in all groups of  $N_g$ .
8.  $d\eta$ -distribution does not depend on  $N_g$ . This observation is in nice agreement with the prediction of energy flux cascade model.
9. The value of mean normalized pseudorapidity density,  $r(\eta)$  is less than unity in projectile fragmentation region, while it is observed to increase in the target fragmentation.

## References

- [1]. Z.V. Anzon et al., Nucl. Phys. **B** 129, 205 (1977).
- [2]. I. Otterlund et al., Nucl. Phys. **B** 142, 445 (1978).
- [3]. M. Kaur and J. M. Kohli, Phys. Ser. 23,272 (1981).
- [4]. H. Khushnood et al., Can. J. Phys. 60, 1523 (1982).
- [5]. M. Irfan et al., Can. J. Phys. 62 230 (1984).
- [6]. Tauseef Ahmad et al., Nuovo Cim. **A**105, 91 (1992).
- [7]. Fu-Nu Liu, Can. J. Phys. 77, 851 (2000).
- [8]. N. N. Abd-Alah et al., Int J. Mod. Phys. **E** 10, 55 (2001).
- [9]. M. Mohery and N. N. Abd-allah, Int. J. Mod. Phys. **E**11,161 (2002).
- [10]. M. Saleem Khan et al., Nuovo Cim. **A**108,147 (1995).
- [11]. M. Saleem Khan et al., Can. J. Phys. 74,651 (1996).
- [12]. Prithipal Singh and H. Khushnood, Int. J. Mod. Phys. **E** 7,659 (1998).
- [13]. K. Gottfried, Proc. Fifth Int. Conf. on high-energy physics and nuclear structure, Uppsola, Sweden, (1973) 79, Phys. Rev. Lett. **B** 73, 32 (1974).
- [14]. B. Anderson, I. Otterlund and E. Stendlund, Phys. Lett. **B** 73, 343 (1978).
- [15]. D. Ghosh et al., Can. J. Phys. 67 (1989) 67.
- [16]. Alma-Ata-Leningrad-Moscow-Tashkent Collaboration, Lebedev Int. Preprints **No. 9**, Moscow, Russia (1974), Yed Fiz. 22, 736 (1975).
- [17]. Y. Afek et al., Proc. Topical meeting on multiparticle production on nuclei at very high energies. Trieste, Italy (1976).
- [18]. Tauseef Ahmad et al., Nuovo Cim. **A** 107, 683 (1994).
- [19]. E. L. Berger et al., Proc. of Topical Meeting on Multiparticle production on Nuclei at Very High Energies, Trieste, (1976).
- [20]. S. A. Azimov et al., Sov. J. Nucl. Phys. English translation 27, 535 (1978).

## Figure Caption.

- [1]. Angular distributions of relativistic charged particles produced in different  $N_g$  bins.
- [2]. Angular distributions of relativistic charged particles in very forward cone ( $\theta < 8^\circ$ ).
- [3]. Dependence of  $\eta$  -distribution on  $N_g$ .
- [4]. Distribution of  $\langle \eta \rangle$  in different  $N_g$  bins.
- [5].  $D(\eta)$ -distribution of relativistic charged particles in different  $N_g$  bins.
- [6]. Rapidity width distributions in different groups of  $N_g$  in 4.5 A GeV/c  $^{12}\text{C}$ -nucleus interactions
- [7].  $D(\eta)$ -distributions of relativistic charged particles in different  $N_g$  bins.
- [8]. Variation of  $r(\eta)$ -distribution with  $N_g$ .

Table 1. Values of front/back ratio for different  $N_g$  bins in C-nucleus reactions at 4.5 A GeV

$N_g$ bins	Front/back
0	$1.81 \pm 3.71$
1	$4.73 \pm 1.73$
2-3	$2.97 \pm 1.40$
4-5	$4.02 \pm 1.18$
6-8	$3.86 \pm 1.41$
$\geq 9$	$3.67 \pm 0.62$
All $N_g$	$3.51 \pm 2.1$

Table 2. Percentage of events with  $D(\eta) \leq 0.9$  for different  $N_g$  bins

$N_g$ bins	0	1	2,3	4,5	6-8	$\geq 9$
Percentage of events	$50.57 \pm 7.0$	$43.8 \pm 9.8$	$45.0 \pm 6.2$	$29.3 \pm 7.0$	$35.0 \pm 9.5$	$53.8 \pm 7.8$

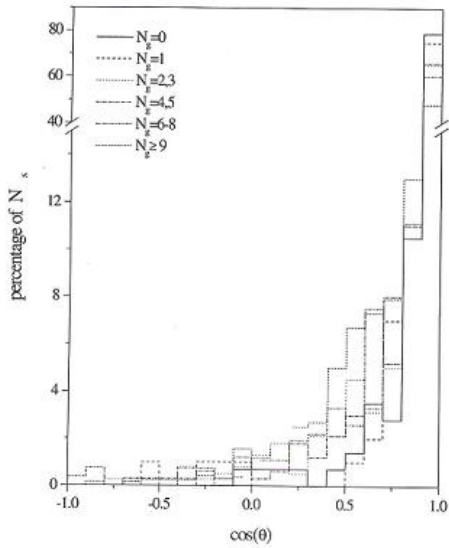


Fig.1

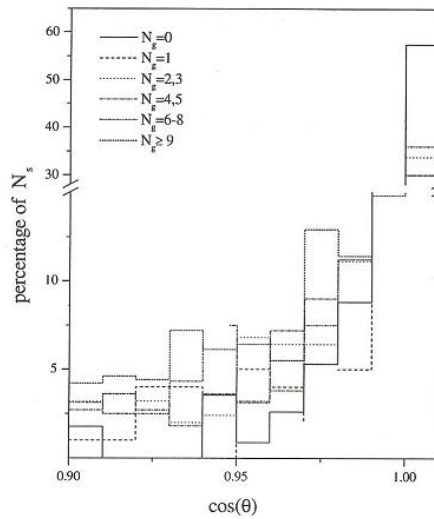


Fig. 2

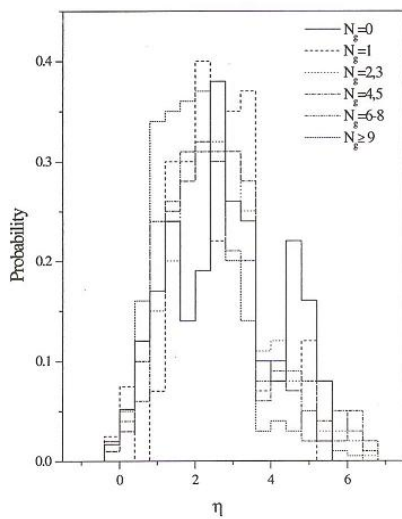


Fig. 3

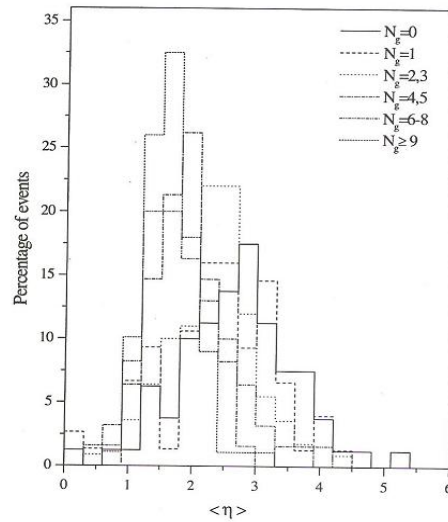


Fig. 4

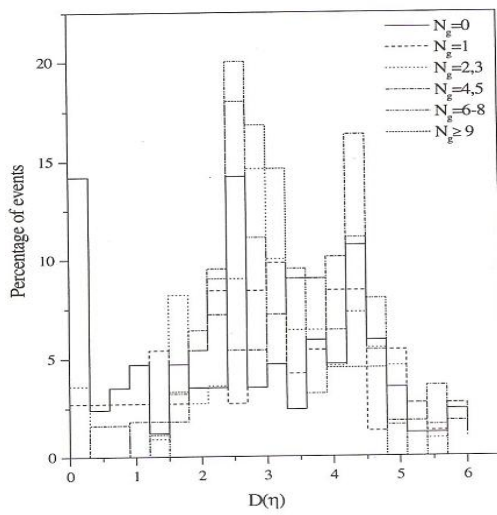


Fig. 5

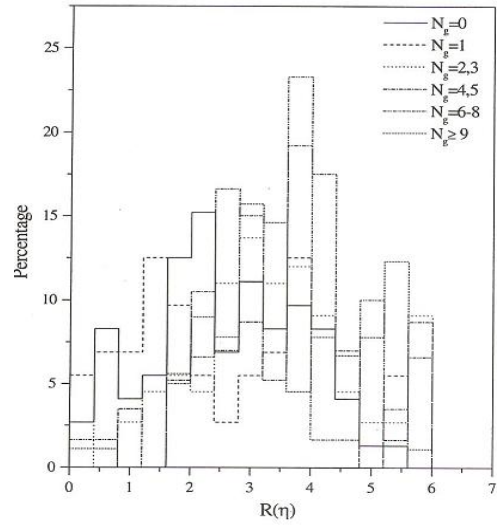


Fig. 6

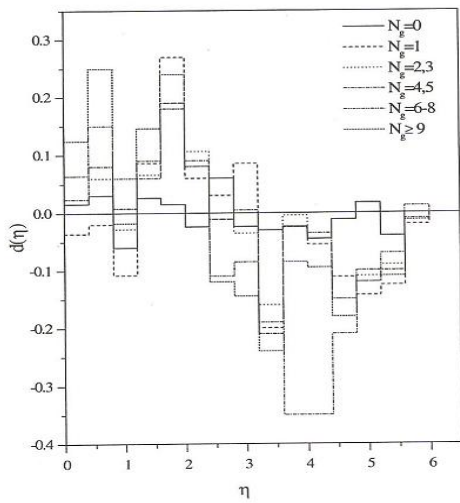


Fig. 7

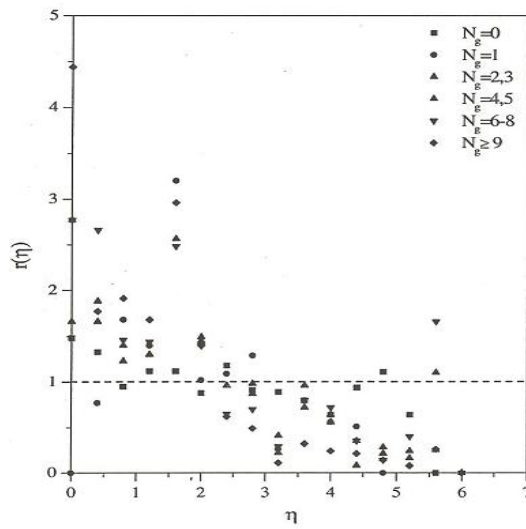


Fig. 8